Peripheral inflammatory injury alters the relative abundance of Gα subunits in the dorsal horn of the spinal cord and in the rostral ventromedial medulla of male rats

Anne-Sophie Wattiez[1], Roxanne Y Walder[1],
Christopher M Sande[1], Stephanie R White[1]
and Donna L Hammond[1,2]

Abstract
A diverse array of G protein-coupled receptors (GPCRs) is implicated in the modulation of nociception. The efficacy and potency of several GPCR agonists change as a consequence of peripheral inflammatory injury. Whether these changes reflect alterations in expression of the G proteins themselves is not known. This study examined the expression of transcripts and proteins for the α subunits of three classes of heteromeric G proteins in the dorsal horn of the spinal cord and the rostral ventromedial medulla (RVM) of male rats four days and two weeks after intraplantar injection of complete Freund's adjuvant (CFA) or saline. Levels of Gα transcript in the dorsal horn or RVM were unchanged by CFA treatment. However, in the dorsal horn, Gα$_i$ protein decreased in cytosolic and membrane fractions four days after CFA treatment. Levels of Gα$_z$ protein decreased in the membrane fraction. Levels of the other Gα subunits did not differ. Levels of the Gα subunits were unchanged two weeks after CFA treatment. In the RVM, Gα$_z$ protein levels decreased in the cytosolic fraction four days after CFA treatment. No other differences were observed. Two weeks after CFA, the levels for all Gα subunits trended higher in the RVM. These data indicate that peripheral inflammatory injury induces subtle changes in the abundance of Gα subunits that is specific with respect to class, subcellular compartment, tissue, and time after injury. These changes have the potential to alter the balance of the different subcellular signaling pathways through which GPCR agonists act to modulate nociception.

Introduction

Guanine nucleotide-binding proteins (G proteins) couple to seven-transmembrane domain receptors (G protein-coupled receptors (GPCRs)) as a heterotrimer of α, β, and γ subunits. They are integral to intracellular signaling induced by a vast array of hormones, neurotransmitters, and chemokines, as well as autocrine and paracrine factors. Multiple isoforms of each G protein subunit (at least 16 different Gα, 5 β, and 12 γ subunits) provide substantial diversity of structure and specificity of coupling (see earlier reviews[1,2–8]). Based principally on the sequence similarity of the Gα subunit, G proteins have been categorized into four different classes: Gα$_{i/o}$, Gα$_{s/olf}$, Gα$_{q/11}$, and Gα$_{12/13}$.

Activation of G proteins occurs upon ligand binding to the GPCR, resulting in the exchange of guanosine diphosphate for guanosine-5′-triphosphate (GTP) on the Gα subunit and dissociation of the heterotrimer into two units, the GTP-bound Gα subunit and Gβγ subunit.[1,8,9] The dissociated GTP-bound Gα subunit and the Gβγ dimer independently engage a myriad of

[1]Department of Anesthesia, University of Iowa, Iowa City, IA, USA
[2]Department of Pharmacology, University of Iowa, Iowa City, IA, USA

Corresponding author:
Donna L Hammond, Department of Anesthesia, University of Iowa, 200 Hawkins Drive 3000 ML, Iowa City, IA 52242, USA.
Email: donna-hammond@uiowa.edu

downstream intracellular effector proteins. These effectors include canonical regulation of various enzymes, small GTPases and ion channels,[3,8,10] and more recently recognized noncanonical actions such as regulation of microtubule dynamics, cytoskeleton, mitosis, cell motility, and organelle function.[11,12]

Research over the past several decades has implicated nearly 50 different families of GPCRs in nociception.[13] A wide variety of GPCR agonists can produce antinociception, alleviate hyperalgesia, or induce hyperalgesia and allodynia following systemic, intracerebral, or intrathecal administration. In addition, peripheral nerve or inflammatory injury that results in enhanced sensitivity to innocuous or noxious stimuli is accompanied by up- or downregulation of GPCRs or changes in receptor affinity in the peripheral or central nervous system (CNS). By comparison, virtually nothing is known about the impact of peripheral injury on the expression of the G proteins that are responsible for transduction and the engagement of subcellular signaling pathways. This study undertook a systematic analysis of the expression of transcript and protein for three different classes of G proteins in the dorsal horn of the spinal cord, which contains the first synapse in afferent pain pathways, as well as in the rostral ventromedial medulla (RVM), a nucleus with a critical role in the bulbospinal modulation of nociception. It further assessed whether peripheral inflammatory injury, produced by intraplantar injection of complete Freund's adjuvant (CFA), altered levels of transcripts or proteins. This study examined $G\alpha_{i1}$, $G\alpha_{i2}$, $G\alpha_{o}$, $G\alpha_{z}$, $G\alpha_{s/olf}$, and $G\alpha_{q/11}$ subunits because they endow the heterotrimeric complex with considerable specificity of action and mediate the effects of both inhibitory and excitatory GPCRs in the CNS. As G proteins are a potential downstream target for therapeutic intervention in disease states,[6,10] insights from these findings could guide future drug development efforts for the relief of persistent pain.

Materials and methods

Animals and inflammatory injury model

Male Sprague-Dawley adult rats (200–350 g, Charles River, Raleigh, NC, USA) were housed in pairs on 1/8th inch corn cob bedding (Cat. No. 7092; Envigo; Indianapolis, IN) in rooms on a 12 h light/dark cycle with water and food ad libitum. All studies were conducted in accordance with the Guide for Care and Use of Laboratory Animals published by the National Institutes of Health and following the guidelines of the International Association for the Study of Pain. The experiments were approved by the University of Iowa Animal Care and Use Committee, and care was taken to minimize the number of animals used and their

suffering. Female rats were not used as the study was initiated before the National Institutes of Health mandated assessment of both genders.

Persistent inflammatory injury was induced by intraplantar injection of CFA. Rats were lightly anesthetized with isoflurane, and the dorso-ventral thickness of the hind paw was measured with digital calipers. The plantar surface of the left hind paw was then injected with 150 μl of CFA (150 μg of *Mycobacterium butyricum*, 85% Drakeol 5NF, and 15% Aralacel A mannide monooleate emulsifier; Cat. No. 344289; Calbiochem; San Diego, CA) or sterile-filtered saline (pH 7.4). The rats were returned to their cages and singly housed for four days or two weeks depending on the experiment. After the rats were euthanized, paw thickness was measured to verify the presence of inflammation. Four days after the injection of CFA, the thickness of the ipsilateral hind paw had increased from 5.4 ± 0.3 to 9.1 ± 0.9 mm ($N = 36$, paired t-test $p < 0.01$). The thickness of the hind paw in the saline-treated cohort was unchanged (5.5 ± 0.2 to 5.7 ± 0.4 mm; $N = 30$; paired t-test $p = 0.1$). Two weeks after injection of CFA, the thickness of the ipsilateral hind paw had increased from 5.5 ± 0.05 to 8.4 ± 0.2 mm ($N = 28$; paired t-test $p < 0.01$), whereas the thickness of the hind paw in the saline-treated cohort was unchanged (5.4 ± 0.05 to 5.3 ± 0.1 mm; $N = 15$; paired t-test $p = 0.43$). Measures of nociception were not made.

Tissue dissection

On the designated test day, the rats were killed by CO_2 inhalation and a 2-mm transverse slice of the brainstem containing the RVM was immediately isolated on ice and frozen on dry ice. To obtain the RVM, a 1.5-mm diameter tissue punch (Harris Unicore, Ted Pella Inc., Redding, CA) was centered on the midline immediately above the pyramid. The remainder of the slice was fixed in 10% formalin containing 30% sucrose to allow the verification of the site of the RVM tissue punch. The L4 and L5 portion of the spinal cord was removed, chilled on an ice-cold platform, and the ipsilateral dorsal horn was excised. For the quantitative polymerase chain reaction (qPCR) experiments, the tissues were stored at $-20°C$ in RNA*later*TM (Ambion, Life Technologies, Carlsbad, CA) until RNA isolation. For the western blot experiments, the tissues were snap frozen in liquid nitrogen and stored at $-80°C$ until protein isolation.

Real-time qPCR analysis

Primer design. DNA oligonucleotide primers were synthesized and purchased from Integrated DNA Technologies (Coralville, IA). Table 1 lists the sequences of the forward and reverse primers for each of the six G protein

Table 1. Primer sequences for RT-qPCR.

Primer	Sequence	Sequence gene bank ID
Actb		NC_005111.3
Forward	5′ – CCG CGA GTA CAA CCT TCT TG – 3′	
Reverse	5′ – GCA GCG ATA TCG TCA TCC AT – 3′	
Gnai1		NM_013145.1
Forward	5′ – GCC ACG GAT ACG AAG AAT GT – 3′	
Reverse	5′ – GTC AGG TCC AGG ATG CAT TT – 3′	
Gnai2		NM_031035.3
Forward	5′ – TCA TCT TCT GTG TCG CCT TG – 3′	
Reverse	5′ – CTT GTT GGC CCC TGT GTA CT – 3′	
Gnao		NM_017327.1
Forward	5′ – AAA CGT TTA TGG CGA GAT GG – 3′	
Reverse	5′ – TTG GCC ACC TAC ATC AAA CA – 3′	
Gnas		BC158589.1
Forward	5′ – GCA GAA GGA CAA GCA GGT CT – 3′	
Reverse	5′ – CCC TCT CCG TTA AAC CCA TT – 3′	
Gnaz		NM_002073.2
Forward	5′ – TGA CGG CCA TCA TCT TCT GT – 3′	
Reverse	5′ – AGG GAG GTG TTG ATG AAC CA – 3′	
Gnaq		NM_031036.1
Forward	5′ – TGA AAA CGT CAC CTC GAT CA – 3′	
Reverse	5′ – TGC TTT GCT CTC CTC CAT TC – 3′	

RT-qPCR: real-time quantitative polymerase chain reaction analysis.

subtypes and for the reference gene, *Actb*. The primers for *Gnai1*, *Gnai2*, *Gnao*, *Gnas*, and *Actb* are described elsewhere[14,15] and were validated by us. Primers for *Gnaz* and *Gnaq* were newly designed. The process for primer design and validation has been previously described by this laboratory.[14] PCR products were cloned according to the manufacturer's protocol (Strata Clone PCR Cloning Kit, Agilent Technologies) and sequenced at the University of Iowa DNA Facility. All primers used in this study amplified a unique species with a sharp melting curve; no primer-dimer products were detected.

RNA isolation and real-time-qPCR. Total RNA was isolated from dorsal horn and RVM tissue as previously described.[14] As in that study, RNA integrity of >9 out of 10 was confirmed for randomly selected samples. Reverse transcription was performed using 100–600 ng of purified RNA and the SuperScript VILO cDNA synthesis kit in a 20 μl reaction volume according to the manufacturer's protocol (Life Technologies, Carlsbad, CA). For qPCR, each well contained the cDNA product generated from 5 ng of input RNA, forward and reverse primers (12 nM for *Actb* and 10 nM for G protein subtypes), and the fluorogenic DNA-binding dye iQ™ SYBR® Green Supermix (Bio-Rad, Hercules, CA) in

20 μl. Reactions were performed in triplicate on a Bio-Rad CFX96 thermocycler (Bio-Rad, Hercules, CA). The cycle conditions were as follows: 50°C for 2 min, 95°C for 10 min followed by 40 cycles (95°C for 15 s, 60°C for 1 min, and 72°C for 1 min), and then 95°C for 1 min and 55°C for 1 min. No-reverse transcriptase and no template controls for each primer set did not amplify any product. Copy number was determined from a five-point standard curve (5-log units) of cloned plasmids containing the target amplicon for each primer set. Transcription efficiencies were similar for all primers and averaged at $E = 99.5\% \pm 0.5$, $r^2 \geqslant 0.997 \pm 0.0002$, slope $= -3.29 \pm 0.06$.

Western blotting

Tissues were homogenized using plastic pestles in an excess of ice-cold lysis buffer (50 mM Tris-HCl pH 8.0, 150 mM NaCl, 1 mM ethylenediaminetetraacetic acid (EDTA), 50 mM NaF, 1 mM NaVO$_3$, 1% Igepal CA-630, and 0.1% sodium dodecyl sulfate (SDS)) supplemented with protease inhibitors (Roche complete Mini protease cocktail; Indianapolis, IN). After centrifugation at 800 *g* for 10 min at 4°C, the resulting supernatant was centrifuged again at 15,000 *g* for 30 min at 4°C. This step yielded an S2 fraction enriched in cytosolic proteins and

Table 2. Sources and specifics of antibodies and blocking peptides used in this study.

Target	RRID	Antibody and antigen sequence	Blocking peptide	Related G protein blocking peptide
$G\alpha_i$	AB_1903980	Cell Signaling 5290S, lot 3 Proprietary; vicinity of Arg100	10/2014 Lot 1 14508S	$G\alpha_o$: sc-387 P
$G\alpha_o$	AB_2111641	Santa Cruz sc-387, lot B261 KMVCDVVSRMEDTEPFSAEL	sc-387 P	Ref: 10/2014 Lot1. 14508S
$G\alpha_{s/olf}$	AB_631539	Santa Cruz sc-383, lot H1211 DQRNEEKAQRE	sc-383 P	$G\alpha_{q/11}$: sc-392 P
$G\alpha_{q/11}$	AB_631537	Santa Cruz sc-392, lot C1915 FAAVKDTILQ LNLKEYNLV	sc-392 P	$G\alpha_{s/olf}$: sc-383 P
$G\alpha_z$	AB_2111817	Santa Cruz sc-388, lot D0314 IDFHNPDRAYDAVQLFALTG	sc-388 P	$G\alpha_o$: sc-387 P

a P2 pellet enriched in membrane proteins. The P2 was resuspended in lysis buffer, and the micro bicinchoninic acid protein assay was used to measure protein concentrations of both the S2 and P2 fractions (Pierce, Rockford, IL). Twenty-five μg of protein was then added to sample buffer (dithiothreitol (DTT), SDS, 1 M Tris pH 6.8, glycerol, bromophenol blue, and lysis buffer), and the samples were heated for 15 min at 65°C. Samples were separated on a TGX gel (Any kD^TM Mini-PROTEAN® TGX Stain-Free^TM Gel, 10 well, 30 μl, BioRad, Hercules, CA) in 1X Laemmli running buffer (Tris base, glycine, SDS, pH 8.3) and transferred to a 0.45 μm polyvinylidene difluoride (PVDF) membrane (Immobilon-P, Merck Millipore Ltd., Cork, Ireland). The membranes were blocked with TBS and 0.1% Tween 20 (TBST) containing 5% nonfat milk for 1 h at room temperature. Membranes were then incubated overnight at 4°C with rabbit polyclonal anti-$G\alpha_o$ (0.2 μg/ml, sc-387), rabbit polyclonal anti-$G\alpha_{q/11}$ (0.2 μg/ml, sc-392), rabbit polyclonal anti-$G\alpha_z$ (0.1 μg/ml, sc-388), or rabbit polyclonal anti-$G\alpha_i$ (16 ng/ml, 5290S) diluted in 5% bovine serum albumin (BSA) in TBST. Membranes were incubated for 1 h at 4°C with rabbit polyclonal anti-$G\alpha_{s/olf}$ (0.2 μg/ml, sc-383). Table 2 provides the sources and specifics about these antibodies. After three rinses with TBST, the membranes were incubated with horseradish peroxidase-linked secondary antibody (goat anti-rabbit sc-2004, 0.2 μg/ ml, lot #H1015, Santa Cruz) diluted in TBST containing 5% nonfat milk for 2 h ($G\alpha_i$, $G\alpha_o$, $G\alpha_{q/11}$, and $G\alpha_z$) or 30 min ($G\alpha_{s/olf}$) at room temperature. After thorough washing with TBST, the membranes were developed with the Western C Chemiluminescent reagent according to manufacturer's instructions (Immun-Star Western Chemiluminescent Kit, BioRad). Images were acquired at multiple exposures to ensure that that oversaturation did not occur and analyzed using the ChemiDoc^TM XRS+ system and Image Lab^TM software (BioRad).

Each gel was loaded with the cytosolic and membrane fractions of a sample from each of the four treatment groups. Stain-free gel technology[16] was used to quantify variations in protein loaded and the signal intensity for the $G\alpha$ subunit was adjusted accordingly. The intensity of the signal was then expressed as a percentage of the total sum of the bands on the blot.[17]

Validation of antibodies

The antibodies used in this study were validated using protein prepared from cortical tissue (Figure 1). The antibody for $G\alpha_i$ recognized a single band of 40.3 kD that was greatly diminished when the antibody was preabsorbed with a 1000 excess of the antigen for $G\alpha_i$ (sc-387 P; Santa Cruz). The large excess was inadvertent because the concentration of the primary antibody was not known until the time of manuscript submission. The antibody for $G\alpha_o$ recognized two bands at 38.8 and 77.2 kD. Unlike the 38.8 kD band, the 77.2 kD band was still detected when the antibody was preabsorbed with a 14-fold excess of its respective antigen sc-387 P. The antibody for $G\alpha_{s/olf}$ recognized a doublet of bands of 45.4 kD and 42.0 kD, both of which were greatly diminished when the antibody was preabsorbed with a 13-fold excess of its respective antigen (sc-383 P, Santa Cruz). The antibody for $G\alpha_{q/11}$ similarly recognized two bands at 38.6 kD and 35.8 kD, both of which were greatly diminished upon preabsorption of the antibody with a 14.6-fold excess of its respective antigen (sc-392 P; Santa Cruz). The antibody for $G\alpha_z$, recognized two bands of 39.5 and 42.3 kD, both of which were greatly diminished upon preabsorption of the antibody with a 28-fold excess of its antigen (sc-388 P; Santa Cruz). Finally, as an additional control, these antibodies were also preabsorbed with excess amounts of the antigen for the $G\alpha$ subunit having the closest related sequence (Table 2). This preabsorption did not eliminate labeling of the appropriate band for any subunit, although signal for $G\alpha_{s/olf}$ and $G\alpha_q$ was slightly diminished.

Statistical analysis

All data are expressed as the mean and SEM. The rank order of the mRNA expression (in copy numbers normalized to copy numbers of *Actb*) of the different G protein gene subtypes was determined by a Kruskal–Wallis test followed by post hoc Mann–Whitney tests in which *p* was corrected for total number of comparisons. For
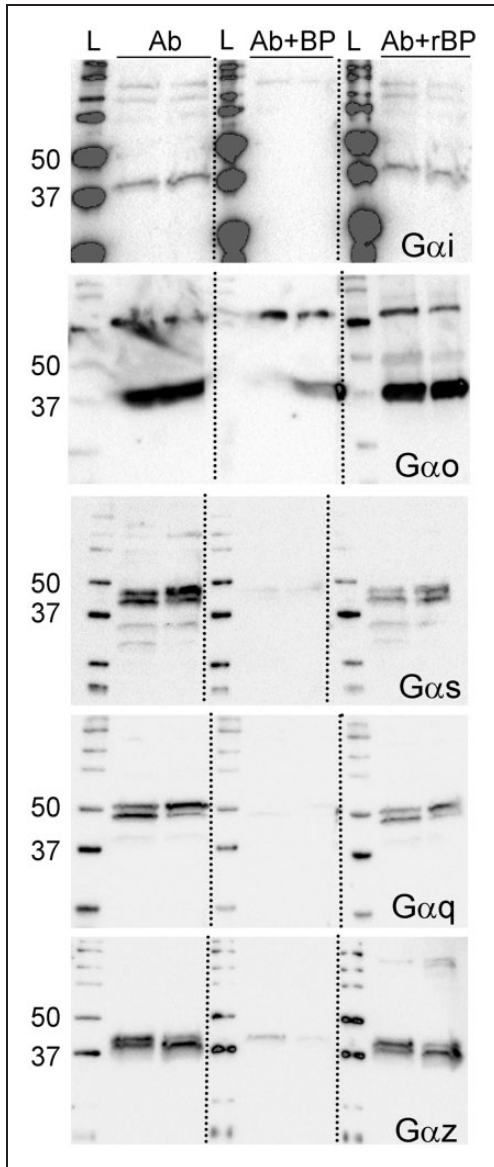
Figure 1. Validation of the specificity of the antibodies for $G\alpha_i$, $G\alpha_o$, $G\alpha_z$, $G\alpha_{s/olf}$, and $G\alpha_{q/11}$ using 25 µg protein obtained from cortex of untreated rats. Conditions were incubation with the antibody alone (left panel), preabsorbed with an excess of antigen (middle panel; BP: blocking peptide), or preabsorbed with at least a 13-fold excess of the antigen for the G protein subunit of closest sequence similarity (right panel; rBP: related blocking peptide). In each panel, the sequence of lanes from left to right is molecular weight ladder (L), cytosolic fraction, and membrane fraction. Dotted lines indicate where blots were cut apart for incubation in the different conditions and then realigned for imaging. Small adjustments to contrast and brightness were applied uniformly.

comparison of transcripts in saline- and CFA-treated rats, results were expressed as $2^{-\Delta Ct}$ (*Actb* served as the reference gene). Levels of *Actb* in the RVM and dorsal horn do not change after CFA treatment and are therefore appropriate for normalization and as a reference

gene.[14] Unpaired *t*-tests or Mann–Whitney tests were used to compare levels of transcript or protein between saline and CFA-treated rats. All statistical tests were two-tailed in nature, and $p < 0.05$ was considered significant. Data were subjected to Grubbs test to identify outliers before analysis. As a result, for determination of relative abundance of transcript, a single value was excluded among *Gnas* in the dorsal horn of two-week saline-treated rats. No values were excluded for comparisons of transcript between saline- and CFA-treated rats. For comparisons of G protein levels, a single value was excluded from each of the following groups in the four-day treatment groups only: dorsal horn—$G\alpha_o$ cytosolic CFA-treated, $G\alpha_o$ membrane CFA-treated, $G\alpha_i$ membrane CFA-treated; RVM—$G\alpha_i$ cytosolic saline-treated, $G\alpha_o$ membrane CFA-treated, $G\alpha_{q/11}$ cytosolic CFA treated.

Results

Transcript levels in the dorsal horn and the RVM of saline-treated rats

Transcripts for *Gnai1*, *Gnai2*, *Gnao*, *Gnas*, *Gnaz*, and *Gnaq* were readily detected in the dorsal horn of saline-treated rats (Figure 2(a)). Aggregation of data from the four-day and two-week treatment groups indicated that levels of *Gnas* transcript were greater than all other G protein subtypes ($p < 0.05$), and about three times greater than the next abundant subtypes, *Gnai2* and *Gnao* ($p < 0.05$). Transcript levels of *Gnai2* and *Gnao* were roughly twice those of *Gnai1* and *Gnaq* ($p < 0.05$), which in turn were ~10 times greater than those of *Gnaz* ($p < 0.05$).

In the RVM, aggregation of data from the four-day and two-week treatment groups indicated that the copy number of *Gnas* transcripts was greater than all other G protein subtypes ($p < 0.01$) and more than twice that of the next abundant subtype, *Gnao* ($p < 0.01$, Figure 2(b)). Levels of *Gnao* transcript were about twice that of *Gnai1* and *Gnai2* ($p < 0.01$). Transcript levels for *Gnai1* were greater than for *Gnaq*, and *Gnaq* was higher than *GNaz*. With respect to differences between the RVM and dorsal horn, levels of transcript for *Gnao*, *Gnas*, and *Gnaz* were greater in the RVM compared to the dorsal horn ($p < 0.01$ for each).

Transcript levels in the dorsal horn and in the RVM of rats with persistent inflammatory pain

Transcripts for *Gnai1*, *Gnai2*, *Gnao*, *Gnas*, *Gnaz*, and *Gnaq* were also readily detected in the dorsal horn and RVM of CFA-treated rats (Figure 3). In the dorsal horn, the levels of transcript for the six different G protein subunits in CFA-treated rats did not differ from their respective values in saline-treated rats at either four days (Figure
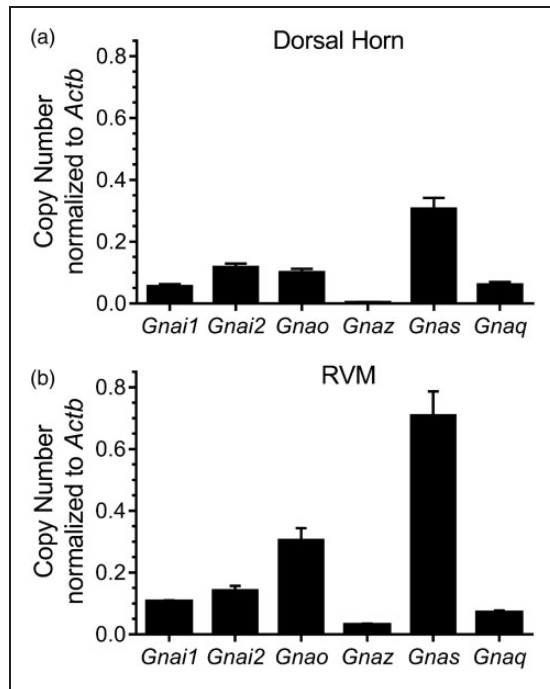
Figure 2. Differential expression of transcripts for *Gnai1*, *Gnai2*, *Gnao*, *Gnas*, *Gnaz*, and *Gnaq* in the dorsal horn (a) and the RVM (b) of rats that received an intraplantar injection of saline four days or two weeks earlier. Results are expressed as copy numbers normalized to copy numbers of *Actb* detected in the same samples. For the dorsal horn, data are mean ± SEM of determinations made in 10 rats (pooled data from five at four days and five at two weeks after treatment). For the RVM, data are the mean ± SEM of determinations made in nine to 13 rats (pooled data from five to six rats at four days and four to seven at two weeks after treatment) for all transcripts except *Gnas*. For *Gnas* in the RVM, the data are the mean ± SEM of determinations in 20 rats (10 at four days and 10 at two weeks after treatment) because greater variability necessitated a larger N. Where standard errors are not visible, they fall within the border of the bar. For dorsal horn, the rank order of abundance is *Gnas* >> *Gnai2* = *Gnao* > *Gnai1* = *Gnaq* >> *Gnaz*. For RVM, the rank order of abundance is *Gnas* >> *Gnao* > *Gnai2* = *Gnai1* = *Gnaq* > *Gnaz*. RVM: rostral ventromedial medulla.

3(a)) or two weeks (Figure 3(b); $p > 0.3$ for all comparisons). Similarly, none of the transcripts in the RVM of CFA-treated rats differed from those in the corresponding saline-treated group at either four days (Figure 3(c)) or two weeks (Figure 3(d); $p > 0.1$ for all comparisons).

G proteins in the dorsal horn of saline- and CFA-treated rats

$G\alpha_i$, $G\alpha_o$, $G\alpha_z$, $G\alpha_{s/olf}$, and $G\alpha_{q/11}$ subunits were detected in the cytosolic and membrane fractions of homogenates of the ipsilateral dorsal horn of both saline- and CFA-treated rats. Comparison of the levels of the different subunits to one another within a treatment condition is not possible because the titers of the respective antibodies are unknown. However, comparisons between CFA- and saline-treated rats can be made for each subunit. The sample size of six rats/group provided sufficient power to detect effect sizes of 1.15 or greater (mean difference of the treatment groups standardized to the pooled standard deviation; Hedge's g).

$G\alpha_i$ protein levels were decreased by 50% in both the cytosolic ($p < 0.05$) and membrane ($p < 0.05$) fractions of the dorsal horn four days after CFA treatment (Figure 4(a) and (c)). $G\alpha_z$ protein levels in the membrane fraction were also decreased by 50% four days after CFA but were unchanged in the cytosolic fraction. Levels of $G\alpha_o$, $G\alpha_{s/olf}$ and $G\alpha_{q/11}$ protein in the dorsal horn of CFA-treated rats did not differ from those of saline-treated rats in cytosolic or membrane fractions at four days ($p > 0.13$ for all comparisons). No significant differences were observed at two weeks for any of the G protein subunits in either fraction (Figure 4(b) and (d); $p > 0.17$ for all comparisons). Examples of blots obtained using dorsal horn tissue from saline and CFA-treated rats are presented in Figure 5.

G proteins in the RVM of saline- and CFA-treated rats

$G\alpha_i$, $G\alpha_o$, $G\alpha_z$, $G\alpha_{s/olf}$, and $G\alpha_{q/11}$ subunits were also readily detected in the cytosolic and membrane fractions prepared from homogenates of RVM tissue from CFA-treated and saline-treated rats (Figure 6). Sample sizes of six to eight were required to obtain sufficient power to detect effect sizes of 1.2 or greater (Hedge's g). Four days after CFA, $G\alpha_z$ subunit ($p < 0.05$) in the cytosolic fraction decreased by about 50% in the absence of a change in levels in the membrane fraction (Figure 6(a) and (c)). Levels of $G\alpha_{s/olf}$ and $G\alpha_{q/11}$ subunit were unchanged in both cytosolic and membrane fractions ($p > 0.09$ for all subunits; Figure 6(c)). Although p values of 0.06 and effect sizes of 1 were obtained for both $G\alpha_i$ and $G\alpha_o$ subunits in the cytosolic fraction four days after CFA (Figure 5(a)), each analysis was powered only to a β of 0.45. An analysis of sample size indicated that an N of 14 would be required to be sufficiently powered to detect the difference. Levels in the membrane fraction were unchanged (Figure 6(c); $p > 0.1$ for each). Two weeks after injection of CFA, cytosolic levels of $G\alpha_i$, $G\alpha_o$, $G\alpha_z$, $G\alpha_{s/olf}$, and $G\alpha_{q/11}$ were unchanged (Figure 6(b); $p > 0.09$ for all subunits). Interestingly, in the membrane fraction of CFA-treated rats, all five G protein subunits trended higher in CFA-treated rats with Hedges g values of 0.73, 0.76, 0.59, 0.94, and 1.15 for $G\alpha_i$, $G\alpha_o$, $G\alpha_z$, $G\alpha_{s/olf}$, and $G\alpha_{q/11}$, respectively. However, p values of 0.06 to 0.2 were obtained, and sample size analysis indicated that sample sizes of between 11 and 25 would be
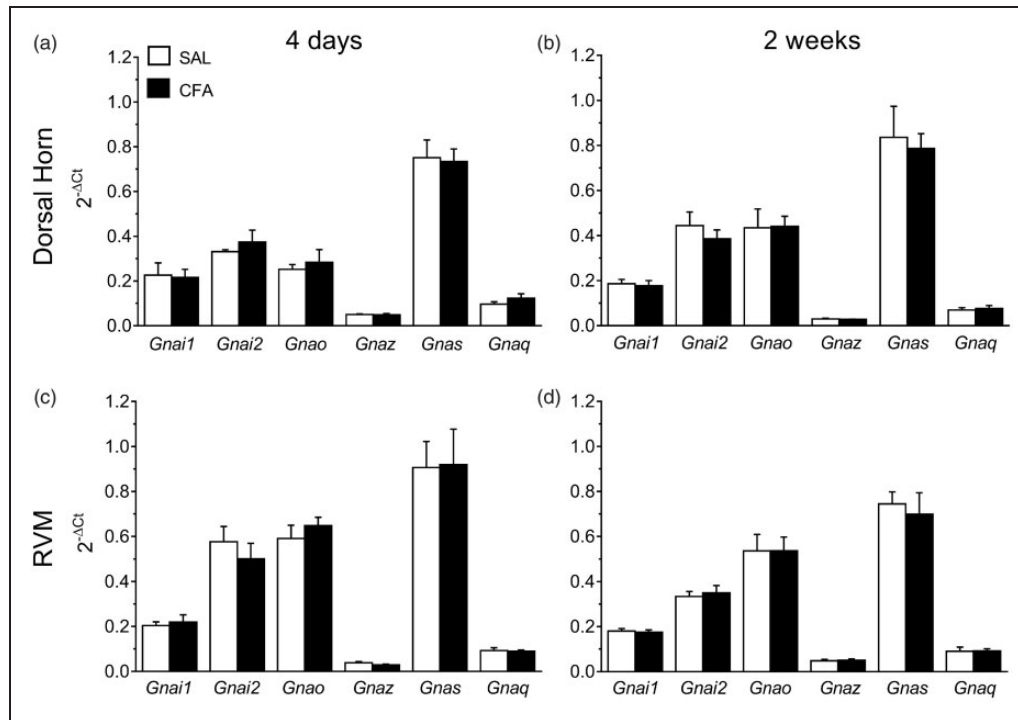
Figure 3. Comparison of transcript levels for the different G protein subtypes in the dorsal horn (a, b) and the RVM (c, d) of rats four days (a, c) or two weeks (b, d) after injection of saline (open bars) or complete Freund's adjuvant (CFA; filled bars). Results are expressed as $2^{-\Delta Ct}$ (*Actb* served as the reference gene). For all transcripts in the dorsal horn, data are the mean $\pm$ SEM of determinations in five rats in each treatment group. For the RVM, data are the mean $\pm$ SEM of determinations in four to seven rats in each treatment group for the RVM, with the exception of *Gnas* for which the *N* was 10 in each treatment group. Transcript levels did not differ between saline- and CFA-treated animals in any group.
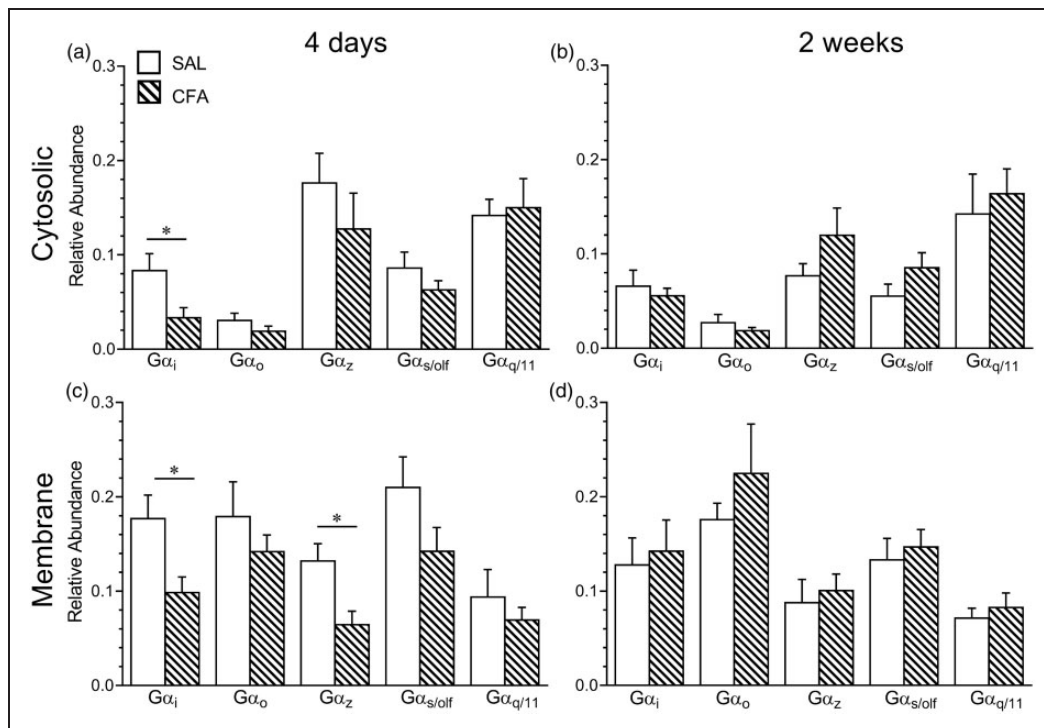RVM: rostral ventromedial medulla.

Figure 4. Levels of the different G protein subunits in the cytosolic (a, b) and membrane (c, d) fractions of the dorsal horn four days (a, c) and two weeks (b, d) after intraplantar injection of saline (open bars) or complete Freund's adjuvant (CFA; hatched bars). Data are the mean $\pm$ SEM of five to six rats. *$p < 0.05$ between saline- and CFA-treated groups (unpaired *t*-test or Mann–Whitney test).
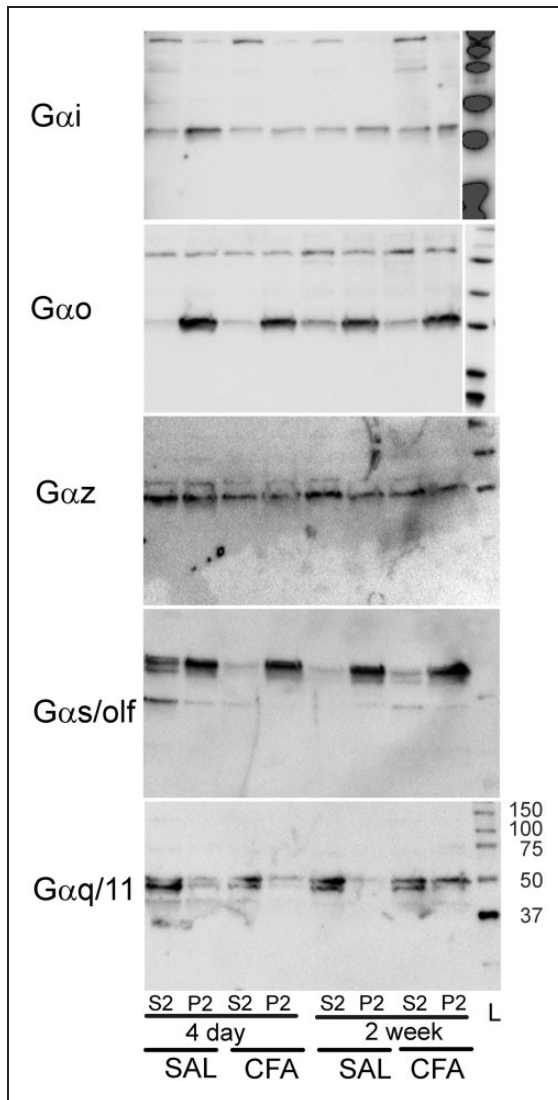
Figure 5. Representative Western blots for each Gα subunit in the dorsal horn. Each blot contains a sample of the cytosolic (S2) and membrane (P2) fraction from one rat four days or two weeks after intraplantar injection of saline or complete Freund's adjuvant (CFA). Each blot is an independent replicate. Stain-free gels were first used to determine total protein loaded on the gel, and immunoreactivity was normalized for differences in the amounts of protein loaded. Immunoreactivity for the subunit was then expressed as a fraction of the total sum of the bands on the blot. L indicates the lane for the molecular weight ladder. For consistency of presentation, the molecular weight ladders for the Gα$_o$ and Gα$_i$ blots were moved from the left to the right of the blot using Photoshop. In the case of Gα$_i$ and Gα$_o$, the higher molecular weight bands did not disappear upon preabsorption of the antibody with the respective antigen. Exposure and gamma were adjusted to −0.22 and 0.6, respectively, for each image.

required to be sufficiently powered to detect these changes. Examples of blots obtained using RVM tissue from saline and CFA-treated rats for each subunit are presented in Figure 7.

Discussion

The Gα subunits of the G protein heterotrimer enable GPCRs to engage a myriad of signaling pathways, endowing GPCRs with a considerable diversity of function. They are also more promiscuous than originally envisioned and can couple to multiple GPCRs albeit with different activation times, affinities, and efficacies.[5,6,18] Even subtle changes in Gα protein localization and levels can have significant ramifications for receptor pharmacology and downstream signaling given the diversity of G proteins that couple to any one GPCR. The present study provides the first systematic examination of the relative abundance of Gα subunit transcripts in two regions of the CNS implicated in the modulation of nociception by a variety of GPCR agonists and additionally documents temporal plasticity in the expression of specific subunits as a result of peripheral inflammatory injury.

Intraplantar injection of CFA produces heat hyperalgesia, mechanical hypersensitivity, and inflammation. The magnitude of heat hyperalgesia and mechanical hypersensitivity changes as a function of time after CFA.[19–21] Also, the efficacy or potency of opioid, glutamatergic, γ-aminobutyric acid, and nicotinic cholinergic receptor agonists in the RVM changes during the two weeks after CFA,[19,22–25] as does the potency of intrathecally administered opioid receptor agonists.[26] In contrast, inflammation is unchanged between four days and two weeks after CFA.[19,21] The changes induced by CFA in the levels of Gα subunit protein, which are also time-dependent in the RVM and dorsal horn, are therefore more likely to relate to mechanisms of nociception rather than inflammation per se.

Peripheral inflammatory injury and the dorsal horn

This study is the first survey of the relative abundance of Gα subunit transcripts in the dorsal horn. Previous studies, which used in situ hybridization histochemistry to map the relative abundance of the different Gα transcripts in the CNS, focused on supraspinal nuclei and did not include the spinal cord. We determined that the dorsal horn expressed very high levels of Gα$_s$; intermediate levels of Gα$_{i1}$, Gα$_{i2}$, and Gα$_o$; and low levels of Gα$_q$ and Gα$_z$ transcripts. The abundance of Gα$_s$ transcript compared to the other Gα subunits mirrors findings in a variety of supraspinal sites.[15,27–29] Persistent inflammatory nociception did not alter the relative abundance or levels of transcript of any of the six Gα subunits in the dorsal horn either four days or two weeks after injection of CFA. Whether this indicates that the Gα subunits are not differentially regulated, or that compensatory changes occur in transcription or stability, cannot be determined.

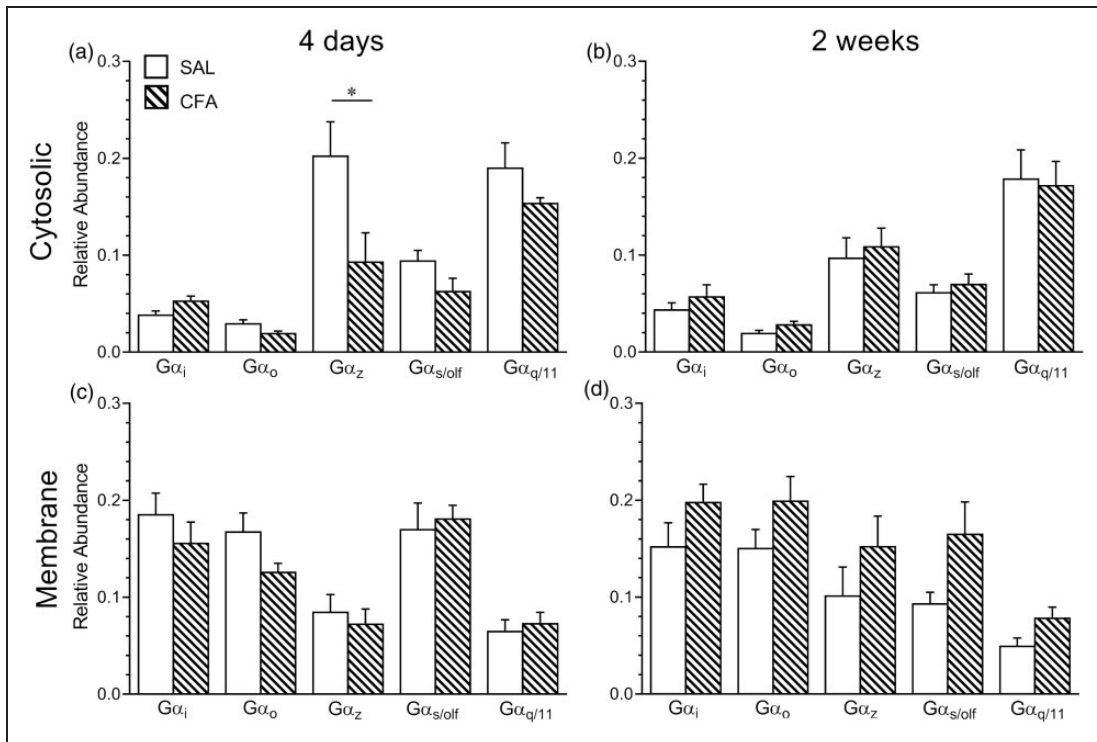In contrast to transcript, the distribution or level of several inhibitory Gα proteins in the dorsal horn was

Figure 6. Levels of the different G protein subunits in the cytosolic (a, b) and membrane (c, d) fractions of the rostral ventromedial medulla (RVM) four days (a, c) and two weeks (b, d) after intraplantar injection of saline (open bars) or complete Freund's adjuvant (CFA; hatched bars). Data are the mean $\pm$ SEM of six to eight rats. *$p < 0.05$ between saline- and CFA-treated groups (unpaired t-test or Mann–Whitney test).

altered following persistent inflammatory injury. These differences likely reflect changes in post-translational processing and were specific with respect to compartment and time. Decreases in $G\alpha_i$ and $G\alpha_z$ were observed only under subacute conditions, assessed four days after CFA treatment. The decrease was evident in both cytosolic and membrane fractions for $G\alpha_i$, whereas it was evident only in the membrane for $G\alpha_z$. This observation is consistent with a loss of inhibition in the dorsal horn and could have a permissive role in the development of heat hyperalgesia and mechanical hypersensitivity after inflammatory injury. The decrease did not persist after chronification of the inflammation (two weeks after CFA injection), suggesting that any dysregulation has been balanced at that stage.

The injury-induced decrease in $G\alpha_i$ and $G\alpha_z$ is likely to affect the actions of a variety of GPCR agonists in the dorsal horn, including those that act at μ, δ, and κ opioid receptors, α_2-adrenergic, cannabinoid, and GABA$_B$ receptors. In the absence of injury, agonists for each of these receptors produce antinociception upon intrathecal administration. Knockdown of $G\alpha_z$ in the dorsal horn of mice results in a loss of potency and efficacy of $\alpha2$-adrenergic receptor agonists (e.g. clonidine), as well as of the delta opioid receptor agonist [D-Pen[2,5]]-enkephalin, but

not the mu opioid receptor agonist morphine[30] (see Standifer et al.[31]). Knockdown of $G\alpha_i$ in the dorsal horn of the mouse diminishes the potency of μ, δ, and κ opioid receptor agonists in the mouse.[31] Given the decrement in both $G\alpha_z$ and $G\alpha_i$ in the dorsal horn of CFA-treated rats, one would expect the effects of agonists at these receptors would be diminished under conditions of persistent inflammatory injury. However, rather than inhibition, the antinociceptive effects of intrathecally administered opioid receptor agonists are enhanced four days after CFA injection.[26] The disconnect between the enhancement of antinociceptive effects of opioid receptor agonists and the decrement in $G\alpha_z$ and $G\alpha_i$ suggests that opioid receptors may switch to engage signaling pathways that are G protein independent under conditions of inflammatory nociception. G protein-coupled receptors can engage multiple signaling pathways through their interactions with β-arrestins and a host of other proteins in addition to G proteins.[32–35] Moreover, different ligands acting at the same receptor can engage different subcellular signaling pathways (i.e. ligand-biased signaling).[35] Therefore, the impact of these changes will be dictated by the extent to which the ligand's action at the receptor is mediated by a G protein-dependent signaling pathway.
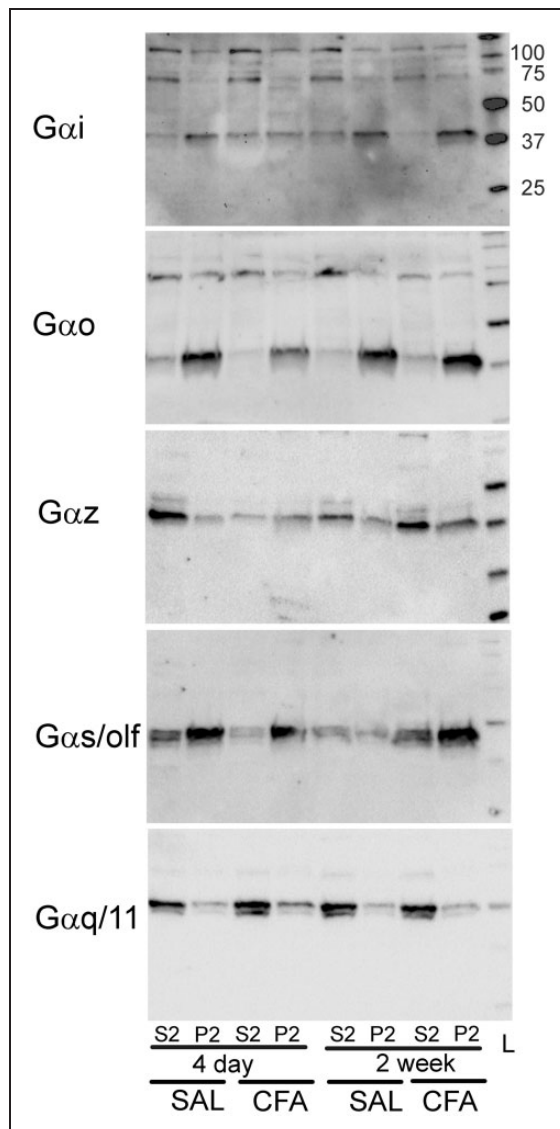
Figure 7. Representative blots for each Gα subunit in the rostral ventromedial medulla (RVM). Each blot contains a sample of the cytosolic (S2) and membrane (P2) fraction from one rat four days or two weeks after intraplantar injection of saline or complete Freund's adjuvant (CFA). Each blot is an independent replicate. Stain-free gels were first used to determine total protein loaded on the gel, and immunoreactivity was normalized for differences in protein loaded. Immunoreactivity for the subunit was then expressed as a fraction of the total sum of the bands on the blot. L indicates the lane for the molecular weight ladder. In the case of Gα$_i$ and Gα$_o$, the higher molecular weight bands did not disappear upon preabsorption of the antibody with the respective antigen. Small adjustments to exposure (−0.22) and contrast (−0.032) were applied uniformly to the images.

Peripheral inflammatory injury and the RVM

This study also provides the first survey of the relative abundance of Gα transcripts in the RVM. The RVM contained very high levels of Gα$_s$; intermediate levels of Gα$_{i1}$, Gα$_{i2}$, and Gα$_o$; and low levels of Gα$_q$ and Gα$_z$ transcripts. The low abundance of Gα$_q$ contrasts with findings made in the rostral ventrolateral medulla.[15] As for the dorsal horn, persistent inflammatory nociception did not alter the relative abundance or levels of transcript of any of the six subunits either four days or two weeks after intraplantar injection of CFA.

Changes in the levels of Gα protein were also observed in the RVM of CFA-treated rats. The only significant effect observed four days after CFA was a decrease in cytosolic levels of Gα$_z$, a pertussis-toxin insensitive G protein. Interestingly, two weeks after CFA, virtually every Gα isoform in the membrane fraction trended upward. Unfortunately, sample sizes of 18 for Gα$_s$, 30 for Gα$_o$, 50 for Gα$_z$, 14 for Gα$_q$, and 40 for Gα$_i$ would be required to detect these differences with a β of 0.8 and α of 0.05. However, given that these samples were run on the same blots as for the four-day treatment groups, the uniform trend is intriguing. At the two-week time point, the actions of μ, δ, and κ opioid receptor agonists in the RVM are enhanced.[19,22] Before dismissing these findings as a lack of effect, it should be noted that if that changes are limited to specific populations of neurons in the RVM, these may not have been apparent when analyzing homogenates. The twofold increase in Gα$_s$ is particularly intriguing as it could provide an additional mechanism for opioids to produce antinociception or antihyperalgesia. Specifically, it could entail a coupling of μ opioid receptors to Gα$_s$ and a direct activation of pain inhibitory neurons, as it has been shown to occur in the dorsal horn of the spinal cord following traumatic neuropathic pain.[36] These findings provide intriguing evidence for possible plasticity in the coupling of Gα proteins to mu opioid receptors following persistent inflammatory injury and to pleiotropic actions of mu opioid receptor agonists. Although this potential mechanism can be addressed by co-immunoprecipitation experiments with the μ opioid receptor and the different Gα protein subtypes, such experiments must await the generation of a suitably specific μ opioid receptor antibody for use in the rat.[37,38]

Regulation of G protein signaling

Other receptors and pathways are likely to be affected by the plasticity that occurs in the RVM and dorsal horn under persistent inflammatory conditions. The determination of which GPCR can bind to which G protein subtype ("fingerprinting") can be determined in heterologous expression systems by bioluminescence resonance energy transfer technology.[5] However, *in vivo*, the cellular environment can strongly influence G protein coupling specificity through changes in the relative abundance of Gα subunits and the sequestering of G proteins by other receptors.[6] Moreover, G protein signaling is

shaped by various regulators like activator of G protein signaling (AGS) themselves, or regulators of G protein signaling (RGS) that can abrogate G protein signaling by accelerating the GTPase activity of Gα.[39]

Gα subunits reversibly shuttle between the cytosolic face of the plasma membrane and the cytosolic surface of endomembranes such as the Golgi, endoplasmic reticulum, endosomes, nuclei, and mitochondria where they can also initiate signaling.[12] Translocation among these different membrane sites would not be detected by Western blotting of the P2 fraction. Changes in the levels of the Gα subunits occurring in one cell compartment (i.e. cytosolic or membrane fraction) were not balanced by the opposite modification in the other compartment, suggesting that internalization to or reinsertion from the cytosol is not responsible for the observed changes. The role of soluble Gα subunits in the cytosol remains poorly understood. An exception is the Gα$_s$ subunit, which is implicated in the regulation of tubulin dynamics and changes in cytoarchitecture.[40] Soluble Gα$_s$ is present in high levels in the cytosol under basal conditions.[41] Unlike any other isoform, Gα$_s$ can undergo endocytosis and distribute to different intracellular compartments following β-adrenergic receptor activation.[41] Finally, heterotrimeric G proteins are also subject to regulation via ubiquitination and degradation.[39] In mammalian cells, ubiquitination of Gα$_s$ makes it a substrate for proteasomal degradation.[42] Modulation of other subtypes has also been shown to depend on the ubiquitination/proteasome system such as Gα$_{i2}$,[43] Gα$_o$,[44] or even Gα$_{i3}$.[45] In the present study, the mechanism responsible for the modulation of the amounts of G protein subtypes in persistent inflammatory conditions could very well be ubiquitin/proteasome dependent, since mRNA levels are unchanged and trafficking does not seem to be involved. The regulatory modulation of G proteins by proteasomal degradation, as well as the function of soluble Gα in inflammatory injury merit further investigation.[46,47]

Conclusion

This study provides important quantitative information on the relative abundance of Gα isoforms in the dorsal horn and the RVM and also demonstrates that neither subacute nor chronic inflammatory nociception alters the expression of transcript. It furthermore provides intriguing evidence for changes in the abundance of various Gα subunits that are specific with respect to subcellular compartment, tissue, and time after injury. These changes could contribute to potential pleiotropic actions of endogenous pain modulatory pathways and to exogenously administered GPCR agonists. Future studies demonstrating coupling of various GPCRs to Gα proteins will be necessary to better assign functionality and to further probe both ligand bias in signaling and pleiotropic actions under conditions of persistent inflammatory nociception.

Author Contributions

ASW and DLH conceived the study, designed the experiments, analyzed the data, and wrote the manuscript. ASW, CMS, RYW, and SRW carried out the experiments. All authors participated in the interpretation of results and read and approved the final manuscript.

Data Access

Data sets and images may be obtained by contacting the corresponding author.

References

1. Albert PR and Robillard L. G protein specificity: traffic direction required. *Cell Signal* 2002; 14: 407–418.
2. Dupre DJ, Robitaille M, Rebois RV, et al. The role of Gbetagamma subunits in the organization, assembly, and function of GPCR signaling complexes. *Annu Rev Pharmacol Toxicol* 2009; 49: 31–56.
3. Jones MB, Siderovski DP and Hooks SB. The G βγ dimer as a novel source of selectivity in G-protein signaling: GGL-ing at convention. *Mol Interv* 2004; 4: 200–214.
4. Khan SM, Sleno R, Gora S, et al. The expanding roles of G βγ subunits in G protein-coupled receptor signaling and drug action. *Pharmacol Rev* 2013; 65: 545–577.
5. Masuho I, Ostrovskaya O, Kramer GM, et al. Distinct profiles of functional discrimination among G proteins determine the actions of G protein-coupled receptors. *Sci Signal* 2015; 8: ra123.
6. Smrcka AV. Fingerprinting G protein-coupled receptor signaling. *Sci Signal* 2015; 8: fs20.
7. Smrcka AV, Oestreich EA, Blaxall BC, et al. EPAC regulation of cardiac EC coupling. *J Physiol* 2007; 584: 1029–1031.
8. Wettschureck N and Offermanns S. Mammalian G proteins and their cell type specific functions. *Physiol Rev* 2005; 85: 1159–1204.
9. Neves SR, Ram PT and Iyengar R. G protein pathways. *Science* 2002; 296: 1636–1639.
10. Smrcka AV. G protein βγ subunits: central mediators of G protein-coupled receptor signaling. *Cell Mol Life Sci* 2008; 65: 2191–2214.

11. Ahmed SM and Angers S. Emerging non-canonical functions for heterotrimeric G proteins in cellular signaling. *J Recept Signal Transduct Res* 2013; 33: 177–183.

12. Hewavitharana T and Wedegaertner PB. Non-canonical signaling and localizations of heterotrimeric G proteins. *Cell Signal* 2012; 24: 25–34.

13. Stone LS and Molliver DC. In search of analgesia: emerging roles of GPCRs in pain. *Mol Interv* 2009; 9: 234–251.

14. Walder RY, Wattiez AS, White SR, et al. Validation of four reference genes for quantitative mRNA expression studies in a rat model of inflammatory injury. *Mol Pain* 2014; 10: 55.

15. Parker LM, Tallapragada VJ, Kumar NN, et al. Distribution and localisation of Galpha proteins in the rostral ventrolateral medulla of normotensive and hypertensive rats: focus on catecholaminergic neurons. *Neuroscience* 2012; 218: 20–34.

16. Taylor SC, Berkelman T, Yadav G, et al. A defined methodology for reliable quantification of Western Blot data. *Mol Biotechnol* 2013; 55: 217–226.

17. Degasperi A, Birtwistle MR, Volinsky N, et al. Evaluating strategies to normalise biological replicates of Western blot data. *PLoS One* 2014; 9: e87293.

18. Oldham WM and Hamm HE. Heterotrimeric G protein activation by G-protein-coupled receptors. *Nat Rev Mol Cell Biol* 2008; 9: 60–71.

19. Hurley RW and Hammond DL. The analgesic effects of supraspinal mu and delta opioid receptor agonists are potentiated during persistent inflammation. *J Neurosci* 2000; 20: 1249–1259.

20. Hamity MV, White SR and Hammond DL. Effects of neurokinin-1 receptor agonism and antagonism in the rostral ventromedial medulla of rats with acute or persistent inflammatory nociception. *Neuroscience* 2010; 165: 902–913.

21. Nagakura Y, Okada M, Kohara A, et al. Allodynia and hyperalgesia in adjuvant-induced arthritic rats: time course of progression and efficacy of analgesics. *J Pharmacol Exp Ther* 2003; 306: 490–497.

22. Schepers RJ, Mahoney JL and Shippenberg TS. Inflammation-induced changes in rostral ventromedial medulla mu and kappa opioid receptor mediated antinociception. *Pain* 2008; 136: 320–330.

23. Gilbert AK and Franklin KB. GABAergic modulation of descending inhibitory systems from the rostral ventromedial medulla (RVM). Dose-response analysis of nociception and neurological deficits. *Pain* 2001; 90: 25–36.

24. Jareczek FJ, White SR and Hammond DL. Plasticity in brainstem mechanisms of pain modulation by nicotinic acetylcholine receptors in the rat. *eNeuro* 2017; 4: 1 e0364.

25. Guan Y, Terayama R, Dubner R, et al. Plasticity in excitatory amino acid receptor-mediated descending pain modulation after inflammation. *J Pharmacol Exp Ther* 2002; 300: 513–520.

26. Hammond DL. Persistent inflammatory nociception and hyperalgesia: implications for opioid actions in the periphery, spinal cord and brainstem. In: Handwerker H and Brune K (eds) *Hyperalgesias – from molecular mechanisms to clinical applications*. Seattle, WA: IASP Press, 2004, pp.291–309.

27. Largent BL, Jones DT, Reed RR, et al. G protein mRNA mapped in rat brain by in situ hybridization. *Proc Natl Acad Sci U S A* 1988; 85: 2864–2868.

28. Brann MR, Collins RM and Spiegel A. Localization of mRNAs encoding the α-subunits of signal-transducing G-proteins within rat brain and among peripheral tissues. *FEBS Lett* 1987; 222: 191–198.

29. Parolaro D, Rubino T, Gori E, et al. In situ hybridization reveals specific increases in $G\alpha_s$ and $G\alpha_o$ mRNA in discrete brain regions of morphine-tolerant rats. *Eur J Pharmacol* 1993; 244: 211–222.

30. Karim F and Roerig SC. Differential effects of antisense oligodeoxynucleotides directed against $G_{z\alpha}$ and $G_{o\alpha}$ on antinociception produced by spinal opioid and α_2 adrenergic receptor agonists. *Pain* 2000; 87: 181–191.

31. Standifer KM, Rossi GC and Pasternak GW. Differential blockade of opioid analgesia by antisense oligodeoxynucleotides directed against various G protein α subunits. *Mol Pharmacol* 1996; 50: 293–298.

32. Georgoussi Z, Georganta EM and Milligan G. The other side of opioid receptor signalling: regulation by protein-protein interaction. *Curr Drug Targets* 2012; 13: 80–102.

33. Raehal KM and Bohn LM. β-arrestins: regulatory role and therapeutic potential in opioid and cannabinoid receptor-mediated analgesia. *Handb Exp Pharmacol* 2014; 219: 427–443.

34. Zheng H, Loh HH and Law PY. Agonist-selective signaling of G protein-coupled receptor: mechanisms and implications. *IUBMB Life* 2010; 62: 112–119.

35. Thompson GL, Kelly E, Christopoulos A, et al. Novel GPCR paradigms at the mu-opioid receptor. *Br J Pharmacol* 2014; 172: 287–296.

36. Largent-Milnes TM, Guo W, Wang HY, et al. Oxycodone plus ultra-low-dose naltrexone attenuates neuropathic pain and associated mu-opioid receptor-Gs coupling. *J Pain* 2008; 9: 700–713.

37. Huang P, Chen C and Liu-Chen LY. Detection of mu opioid receptor (MOPR) and its glycosylation in rat and mouse brains by western blot with anti-μC, an affinity-purified polyclonal anti-MOPR antibody. *Methods Mol Biol* 2015; 1230: 141–154.

38. Schmidt Y, Gaveriaux-Ruff C and Machelska H. μ-Opioid receptor antibody reveals tissue-dependent specific staining and increased neuronal μ-receptor immunoreactivity at the injured nerve trunk in mice. *PLoS One* 2013; 8: e79099.

39. Wang Y and Dohlman HG. Regulation of G protein and mitogen-activated protein kinase signaling by ubiquitination: insights from model organisms. *Circ Res* 2006; 99: 1305–1314.

40. Schappi JM, Krbanjevic A and Rasenick MM. Tubulin, actin and heterotrimeric G proteins: coordination of signaling and structure. *Biochim Biophys Acta* 2014; 1838: 674–681.

41. Martin BR and Lambert NA. Activated G protein $G\alpha_s$ samples multiple endomembrane compartments. *J Biol Chem* 2016; 291: 20295–20302.

42. Naviglio S, Pagano M, Romano M, et al. Adenylate cyclase regulation via proteasome-mediated modulation of $G\alpha_s$ levels. *Cell Signal* 2004; 16: 1229–1237.

43. Ogasawara J, Sakurai T, Rahman N, et al. Acute exercise alters Gαi2 protein expressions through the ubiquitin-proteasome proteolysis pathway in rat adipocytes. *Biochem Biophys Res Commun* 2004; 323: 1109–1115.

44. Busconi L, Guan J and Denker BM. Degradation of heterotrimeric Gα$_o$ subunits via the proteosome pathway is induced by the HSP90-specific compound geldanamycin. *J Biol Chem* 2000; 275: 1565–1569.

45. Fischer T, De Vries L, Meerloo T, et al. Promotion of Gαi3 subunit down-regulation by GIPN, a putative E3 ubiquitin ligase that interacts with RGS-GAIP. *Proc Natl Acad Sci U S A* 2003; 100: 8270–8275.

46. Ang R, Opel A and Tinker A. The role of inhibitory G proteins and regulators of G protein signaling in the in vivo control of heart rate and predisposition to cardiac arrhythmias. *Front Physiol* 2012; 3: 96.

47. Asano T, Semba R, Kamiya N, et al. Go, a GTP-binding protein: immunochemical and immunohistochemical localization in the rat. *J Neurochem* 1988; 50: 1164–1169.